Materials Today: Proceedings 46 (2021) 651–657

Contents lists available at ScienceDirect

Materials Today: Proceedings

journal homepage: www.elsevier.com/locate/matpr

Impact of multi-pass friction stir processing on microhardness of AA1050/AA6082 dissimilar joints

Oritonda Muribwathoho *, Velaphi Msomi, Sipokazi Mabuwa, Sharon Saasebeng Motshwanedi

Cape Peninsula University of Technology, Mechanical Engineering Department, Bellville 7535, South Africa

ARTICLE INFO

Article history:
Received 8 September 2020
Accepted 18 November 2020
Available online 20 January 2021

Keywords:
Friction stir welding
Friction stir processing
Tensile properties
Microhardness
Microstructural analysis

ABSTRACT

The AA1050 and AA6082 aluminum plates were used to produce a dissimilar joint using the friction stir welding (FSW) technique. The produced dissimilar joint was then processed. The processing used is the multi-pass friction stir processing (FSP). Different tests were then conducted on the processed AA1050-AA6082 joints. The results on microstructural analysis revealed that as the number of FSP passes were increased the grain sizes reduced. The ultimate tensile strength of the multi-pass increased with a decrease in elongation as compared to that of a single pass with the same material positioning AA1050-AA6082 joints. For the surface morphology, the fracture surfaces were characterized by dimples on both the first and fourth pass. As the number of passes increased it was noticed that the dimples became smaller. The microhardness was found to have a minor dependency on the number of FSP passes.

1. Introduction

Aluminum alloys, in general, are used in different industries including food packaging aerospace, marine, and automotive industries [1],. Various aluminum alloys possess different mechanical and thermal properties and these differences are influenced by alloying elements used in producing each alloy. Aluminum alloy 6082-T6 is an Al-Mg-Si alloy consisting of sufficient plasticity for extrusions and contains very high relative strength. Aluminum alloy 6082-T6 has excellent weldability, formability, and machinability and is mostly used in the manufacturing of high-speed trains [2,3],[4]. Aluminum alloy 1050-H14 is a grade consisting of moderate strength with excellent corrosion resistance, high ductility, and a reflective appearance. Aluminum alloy 1050-H14 is mostly used in industries like food industries for containers, lamp reflectors, etc. [5].

Friction stir processing (FSP) is an emerging surface-engineering technology, which uses the principle of friction stir welding to process material in a variety of ways besides joining them [6,7]. Friction stir processing was derived from friction stir welding (FSW) developed by the TWI ltd, Cambridge, UK in 1991 [8,9]. FSP has been proven to be an effective technique to achieve major microstructural refinement, densification, and homogeneity of the processed zone, as well as, elimination of defects from manufacturing processes [10–12],[13]. The recent works have demonstrated that FSP can be successfully used for microstructural modification which influences various properties like corrosion resistance, tensile strength, superplasticity, ductility, and wear resistance. Moreover, FSP can be used to produce surface composites, removal of defects, and production of special alloys [14,15].

The recent developments on FSP technology have demonstrated that FSP can be applied on the surface of the material repeatedly and that is termed multi-pass FSP. The recent developments on multi-pass FSP have demonstrated that this technology can be applied on cast [16,17], wrought [18,19], aluminum alloys, copper [20], magnesium alloys [21], titanium [22], and many more. The most investigated properties of the multi-pass friction stir processed plate include mechanical properties, microstructure, hardness, and corrosion [18].

E1-Raves and E1-Danaf [23], analyzed the influence of multi-pass friction stir processing on the microstructural and mechanical properties of aluminum alloy 6082. They discovered that the increase in the number of passes plays a significant role in grain refinement. They also discovered that the ultimate tensile strength and microhardness are improving with the increase in the number of FSP passes. The improvement of these mechanical properties was attributed to the grain refinement. Mirjavadi et al. [24],

* Corresponding author.
E-mail address: oritondamuribwathoho@gmail.com (O. Muribwathoho).

https://doi.org/10.1016/j.matpr.2020.11.587
2214-7853/

Moustafa [25], studied the effect of multi-pass friction stir processing on the microstructure, mechanical and wear properties of AA5083/ZrO2 nanocomposites and effect of multi-pass friction stir processing on mechanical properties for AA2024/Al2O3 nanocomposites, Materials. They discovered that grain refinement occurred with increasing the number of FSP. Moreover, owing to the thermal expansion mismatch between these second-phase particles and the matrix, the density of dislocations increased, and as a result, the hardness values were improved [26].

El-Rayes and El-Danaf [23], studied the influence of multi-pass friction stir processing on the microstructural and mechanical properties of Aluminum Alloy 6082. The found that multi-pass FSP on the AA6082 surface resulted in equiaxed grains comprising of high angle grain boundaries due to dynamic recrystallization

Table 1
Chemical compositions of the dissimilar aluminum alloys [27,28].

	Al	Mg	Zn	Si	Mn	Fe	Cu	V
AA1050	Bal	0.05	0.05	0.05	0.05	0.4	0.05	0.05
AA6082	Bal	1.1	0.20	0.90	0.70	0.50	0.1	–

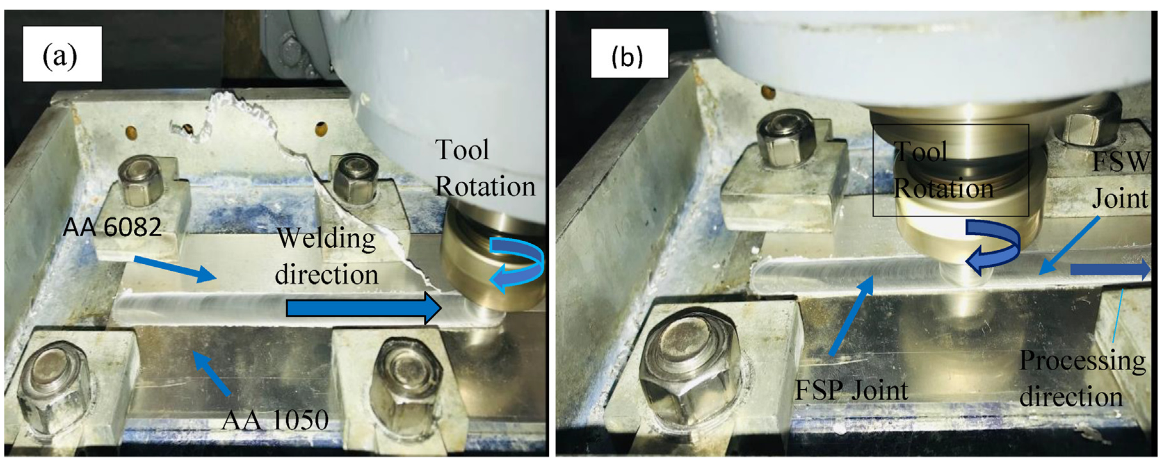

Fig. 1. (a) Friction stir welding with AA1050 on the advancing side, and (b) Friction stir processing.

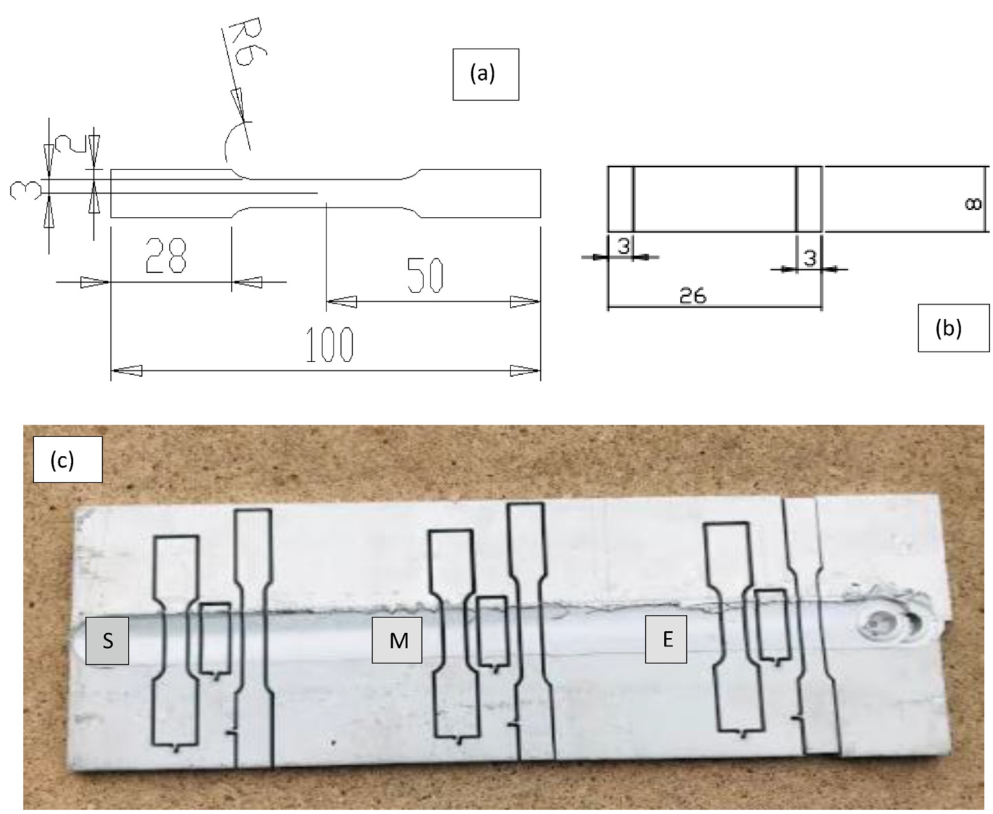

Fig. 2. (a) Tensile test specimen, (b) Microhardness specimen (all the dimensions are in mm) and (c) Specimen position.

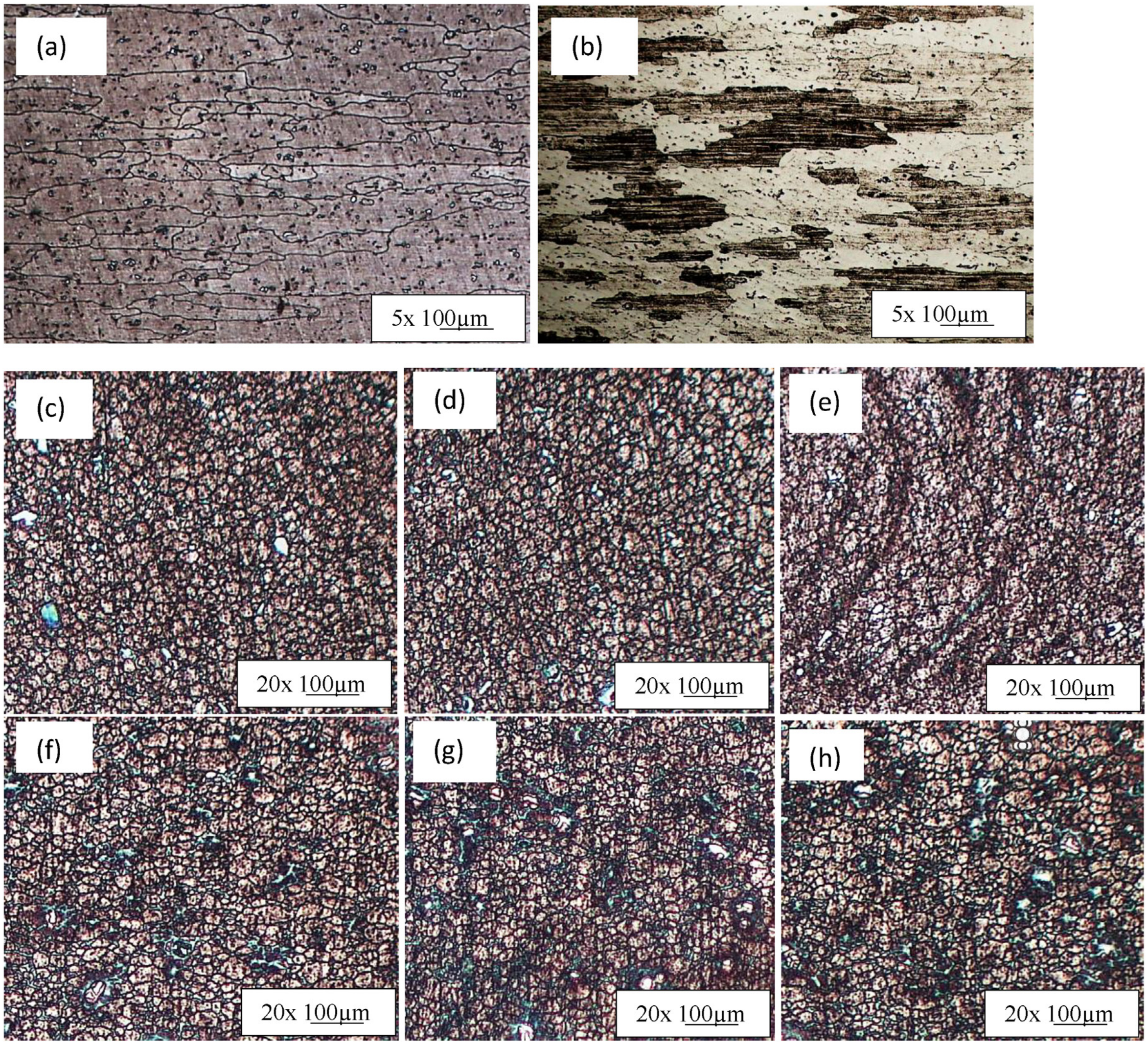

Fig. 3. Micrographs (a) Base material AA6082-T651, (b) Base material AA1050-H14; 1P FSPed AA1050/AA6082 (c) Start, (d) Middle, (e) End; 4P FSPed AA1050/AA6082 (f) Start, (g) Middle and (h) End.

Table 2
Grain sizes and standard deviation.

FSP Joint	Mean values (μm)	Standard deviation
AA1050-6082	125.87	16.53
AA6082-1050	123.19	22.94
1P AA1050/AA6082		
Start	14.84	3.419
Middle	19.18	3.225
End	17.81	3.179
4P AA10/AA6082		
Start	16.62	3.355
Middle	10.75	2.177
End	8.614	2.043

that occurred in the stir zone. An increase in the grain size and fragmentation of second phase particles was noted to be as a result of the heat accumulated during the multi-pass FSP. Additionally, the tensile strength decreased with an increase in the number of FSP passes. The hardness also decreased due to the softening of the material as the number of passes increased.

It has been observed that the majority of multi-pass FSP works focused on the processing of the plates than the joints. There are very few works reporting on multi-pass FSP joints. This paper reports on the impact of the multi-pass FSP technique on the microhardness of AA1050/AA6082 dissimilar joints. The investigation is mainly focusing on the first and the fourth pass.

2. Materials and methods

For this study, AA1050-H14 and AA6082-T651 dissimilar plates with a thickness of 6 mm were used. The chemical compositions of the two dissimilar aluminum alloys are shown in Table 1. Before the application of FSW, the dissimilar plates were cut into the dimensions of 260 × 52 mm to fit the FSW backplate. Two sets from each dissimilar plate were dimensioned and friction stir welded. Fig. 1(a) shows the performance of friction stir welding where AA1050 was positioned on the advancing side while the performance of FSP is shown in Fig. 1(b). The FSW was used to fabricate AA1050/AA6082 dissimilar joint which was then subjected to one-pass (1P) and four-pass (4P) FSP. The parameters used were a tool rotational speed of 1200 rpm, tool traverse speed of 60 mm/min, tool tilt angle of 2°. It should be noted that the same parameters used in processing were also used in FSW. It should be also noted that AA1050/AA6082 means that AA1050 was positioned on the advancing side during FSW and FSP.

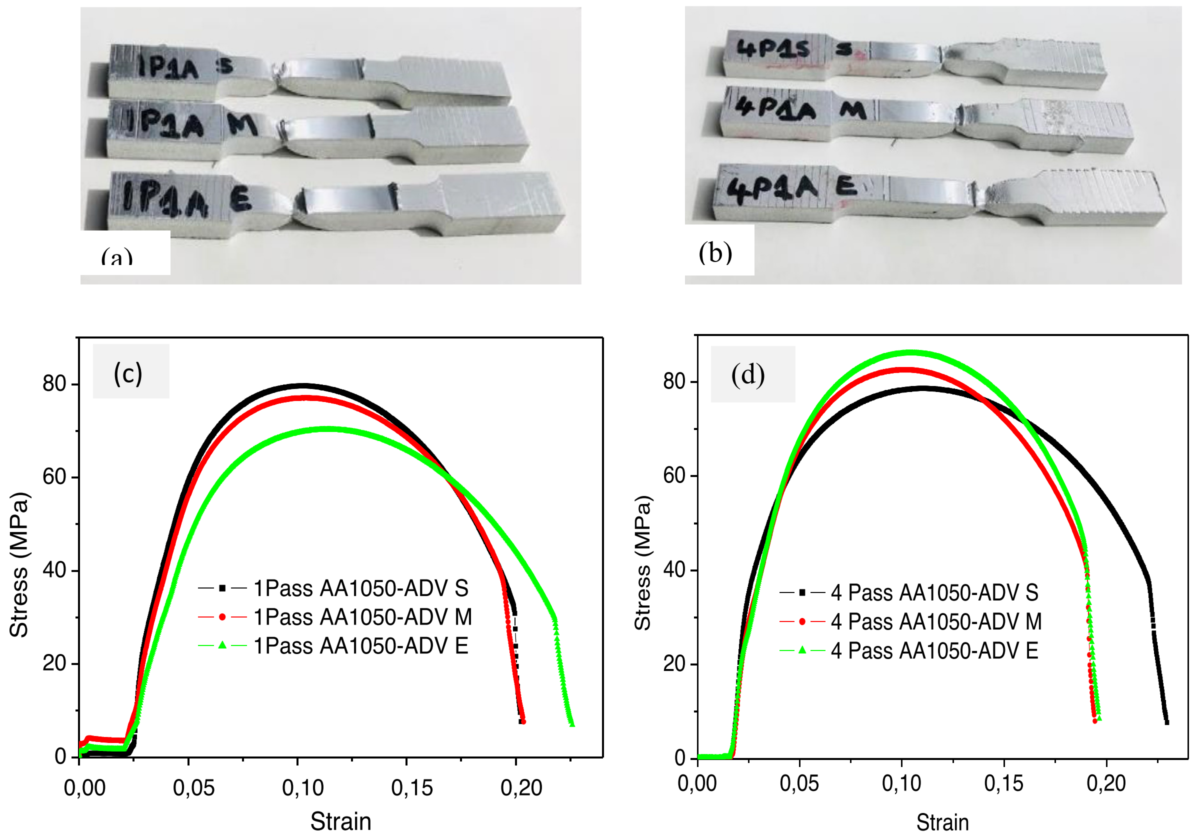

Fig. 4. Post tensile specimens (a) 1P FSPed AA1050/AA6082 (b) 4P FSPed AA1050/AA6082; Stress-Strain curves (c) 1P FSPed AA1050/AA6082 and (d) 4P FSPed AA1050/AA6082.

The waterjet cutting technology was used to cut the friction stir processed plates (FSPed) for different tests. The tests that were conducted include tensile tests, microstructural analysis, and microhardness. The post tensile test specimens were further analyzed for the nature of fracture using a scanning electron microscopy (SEM).

The tensile tests were performed using the Hounsfield 50 K tensile testing machine. The ASTM-E8M-04 standard was used for the tensile specimen geometry and in conducting the tensile test. Fig. 2 (a) shows the schematic diagram of the tensile specimen used for this study. The microhardness was performed using Innova Test (Falcon 500) machine following the ASTM E384-11 standard. The schematic diagram for the specimen used for microhardness is shown in Fig. 2(b). Fig. 2(c) shows the specimen sampling locations. The labels used were S, M, E to mark the start, middle, and end of the friction stir processed joints respectively.

The microstructural metallographic analysis was performed using the Motic AE2000 microscope. The cross-sections surface of the friction stir processed joints were ground, polished then etched. The etchants used for microstructural analysis were modified Keller's reagent and Weck's reagent. The ASTM E112-12 standard was used to determine the average grain size through the ImageJ software.

3. Results and discussion

3.1. Metallographic morphology

The microstructure of the base materials, 1P FSPed AA1050/AA6082, and 4P FSPed AA1050/AA6082 are shown in Fig. 3(a)-(h). Fig. 3(a) shows the microstructure of AA6082 base material while that of AA1050 is shown in Fig. 3(b). The macrographs of the specimens sampled from the start, middle, and end of the 1P friction stir processed (FSPed) AA1050/6082 joint are shown in Fig. 3(c), (d), and (e). Fig. 3(f), (g), and (h) show the microstructure for the specimens sampled from the start, middle, and end of the 4P FSPed AA1050/AA6082. The mean grain sizes and their respective standard deviations of the surfaces depicted in Fig. 3(a)-(h) are shown in Table 2. The AA6082 base material had a mean value of 125.87 μm and a standard deviation of 16.53 while the AA1050 base material had a mean value of 123.19 μm and a standard deviation of 22.94. The mean grain size of 1P FSPed AA1050/AA6082 joint ranged from 14.84 μm to 19.18 μm while the range of 4P FSPed AA1050/AA6082 joint was from 8.61 μm to 16.62 μm. The calculated mean grain size for the processed joint was very close to the individual grain size found at the measured joints and this is judged from the low standard deviation. It was observed that as the number of FSP passes increased the grain sizes decreases. The decrease in grain size with the increase in the number of FSP passes is caused by the repeated dynamic recrystallization experienced by the joint subjected to multi-pass FSP [18,29–31].

Table 3
Tensile properties.

Joint type & sampling position	Ultimate tensile strength (MPa)	Percentage elongation (%)	Position of fracture
1P AA1050/AA6082 S	79.7	19.97	HAZ
1P AA1050/AA6082 M	77.1	19.65	HAZ
1P AA1050/AA6082 E	70.3	21.88	HAZ
4P AA6082/AA8011 S	78.6	22.22	HAZ
4P AA1050/AA6082 M	82.6	19.05	HAZ
4P AA1050/AA6082 E	86.1	18.97	HAZ

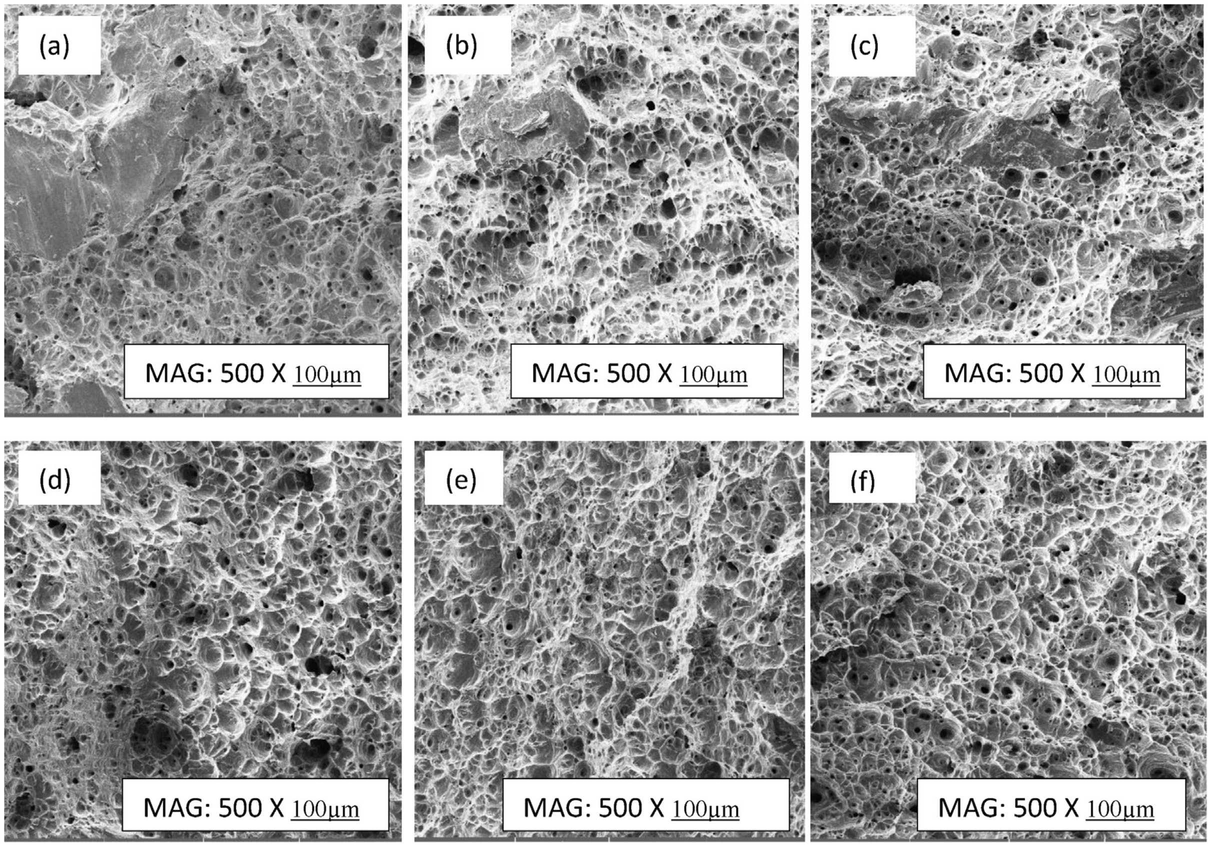

Fig. 5. SEM tensile; 1P FSPed AA1050/AA6082 (a) Start, (b) Middle. (c) End; 4P FSPed AA1050/AA6082 (d) Start, (e) Middle, (f) End.

3.2. Tensile properties

Fig. 4(a) and (b) show fractured specimens post tensile testing while the stress–strain curves for their respective specimens are shown in Fig. 4(c) and (d). The tensile properties in relation to Fig. 4 are presented in Table 3. It was observed that all the specimens failed consistently outside the joint towards the AA1050 side irrespective of the number of FSP passed. The FSPed specimens are bound to fail in this region as it is always dominated by the coarsened grains due to heat produced during the FSP process and this region is termed heat-affected zone (HAZ) [18,27–31]. The ultimate tensile strength (UTS) for the 1P FSPed joint decreased from the start to the end of the joint, however, the percentage elongation was found to be increasing from the start to the end of the joint. The maximum UTS for the 1P FSPed AA1050/AA6082 joint was obtained from the specimen sampled at the start of the joint. The decrease in UTS along the 1P FSPed AA1050/AA6082 joint is attributed to the grain size variation that was observed during microstructural analysis [17,20]. The UTS of the 4P FSPed AA1050/AA6082 joint increased along with the joint, however, the percentage elongation decreases with the increase in UTS for the same joint. This behavior is caused by the decrease in grain size along the 4P FSPed AA1050/AA6082 joint [33,34]. The maximum UTS obtained from the 1P FSPed AA1050/AA6082 joint was 75.9% to that of AA1050 base material and 28.5% to that of AA6082 base material. The percentage elongation for 1P FSPed AA1050/AA6082 joint more than 100% to that of both base materials. The maximum UTS obtained for the 4P FSPed AA1050/AA6082 joint was 30.8% to that of AA6082 base material and 82% to that of AA1050 base material. The percentage elongation for the 4P FSPed AA1050/AA6082 joint was also more than 100% to that of both AA1050 and AA6082 base materials.

3.2.1. Tensile surface morphology

The fractographs of the fractured tensile specimens are shown in Fig. 5. Fig. 5(a)–(c) shows the morphology of the fractured surface for the specimens sampled from the start, middle, and the end of 1P FSPed AA1050/AA6082 joint. Fig. 5 (d)–(f) shows the surface morphology of the fractured surface for the specimens sampled from the start, middle, and end of 4P FSPed AA1050/AA6082. The fractured surface is characterized by the presence of dimples on both the 1P and 4P FSPed AA1050/AA6082 joint (see Fig. 5 (a)-(f)). It was noticed that the dimple size gets reduced with the increase in the number of passes and this phenomenon is influenced by the enhancement of the tensile properties [35].

3.3. Microhardness

Fig. 6 illustrates the microhardness profiles for the FSPed AA1050/AA6082 joints. The microhardness results for the specimens sampled from the start, middle, and end of the 1P FSPed AA1050/AA6082 joint are shown in Fig. 6(a), (c), and (e). The microhardness for the stir zone (SZ) of the 1P FSPed AA1050/AA6082 joint ranged from 65 to 70HV. The maximum SZ microhardness was measured on the specimen sampled from the end of the 1P FSPed AA1050/AA6082 joint. It is worth noting that the very same specimen with maximum microhardness possessed lower tensile strength. The increase in microhardness of this specimen can be linked to the precipitate and the nucleation of thick intermetallic compounds due to high temperature and high deformation rate [18,23,36]. Fig. 6(b), (d), and (f) shows the microhardness profiles for specimens sampled from the start, middle, and end of the 4P FSPed AA1050/AA6082 joint. The SZ microhardness for the said joint ranged from 52 and 55 HV. The maximum SZ microhardness was measured from the

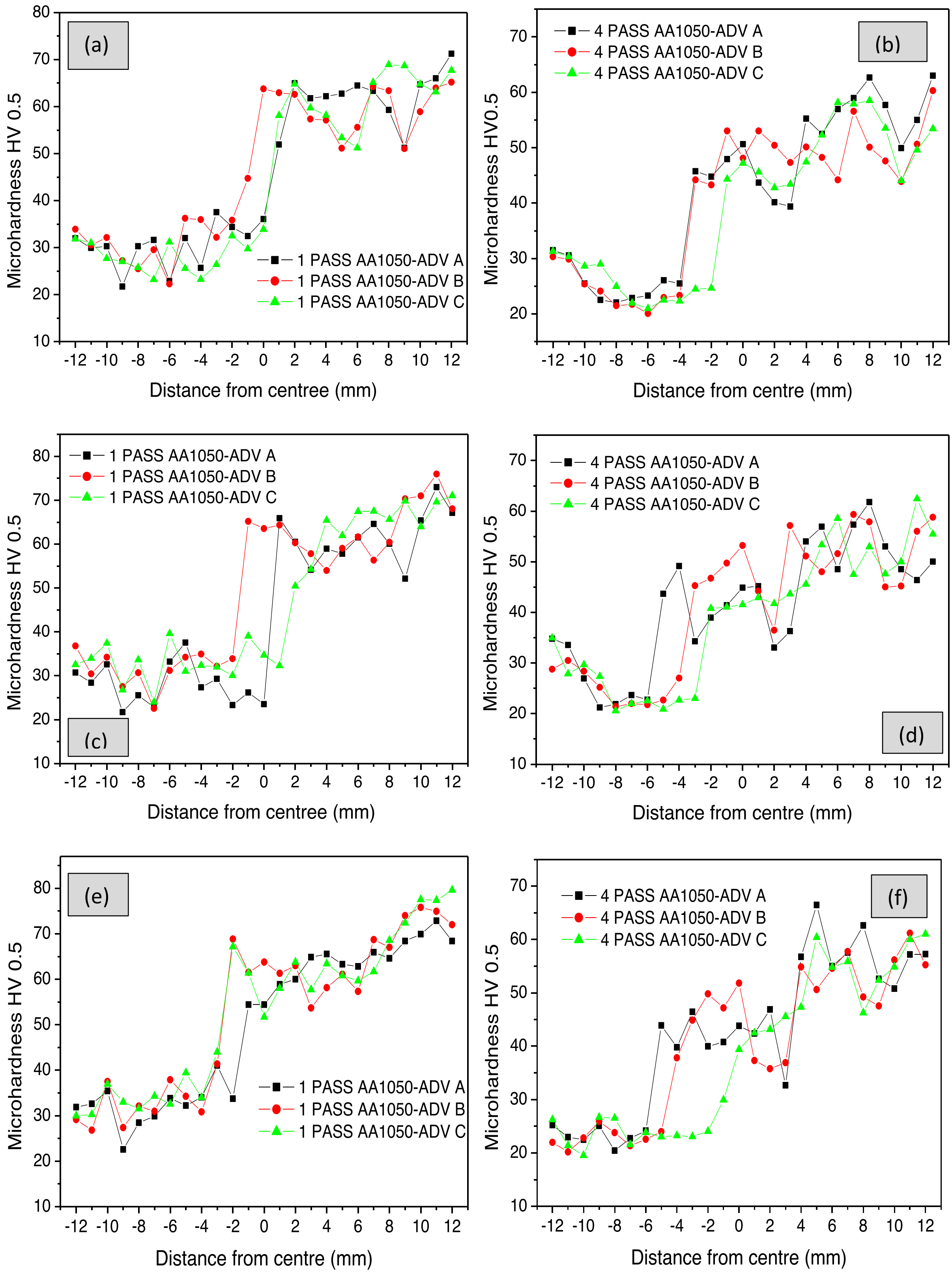

Fig. 6. Microhardness results: 1P FSPed AA1050/AA6082 (a) Start, (c) Middle, (e) End), 4P FSPed AA1050/AA6082 (b) Start, (d) Middle (f) End.

specimens sampled from the start and the middle of the 4P FSPed AA1050/AA6082 joint. The tensile strength of these two specimens was lower compared to the specimen sampled at the end of the same joint. The increase in microhardness of the low UTS specimens is caused by the same phenomenon observed on 1P FSPed AA1050/AA6082 joint [37].

4. Conclusions

The impact of multi-pass friction stir processing on microhardness of AA1050/AA6082 dissimilar joint was conducted successfully. The 1P FSP results were studied comparatively with that of the 4P FSP results. Based on the results obtained, the following conclusions were drawn:

- The grain refinement increased with the increase in the number of FSP passes. The grain refinement led to the enhancement of the tensile strength of the joint with a compromise in percentage elongation. However, the percentage elongation of both joints was found to be more than 100% compared to that of both base materials.
- The microhardness of the specimens with low tensile strength was found to be higher compared to the microhardness of the specimens with higher tensile strength. This phenomenon was similar to that reported in the literature.
- The performance of multi-pass FSP with the weaker material on the advancing side yielded an enhanced percentage elongation than UTS.

Funding

Funding The authors would like to acknowledge the National Research Foundation (NRF) Thuthuka Grant for funding this study.

Declaration of Competing Interest

The authors declare that they have no known competing financial interests or personal relationships that could have appeared to influence the work reported in this paper.

Acknowledgements

The authors would like to thank Miranda Waldron from the SEM department of the University of Cape Town for use of the SEM equipment.

References

[1] G. Selvaraj, T. Karthikeyan, R. Mohanadass, S. Indhumath, Int. J. Appl. Eng. Res. 10 (13) (2015) 11095–11100.
[2] Y. Birol, Mater. Sci. Technol. 31 (2015) 207–211.
[3] Y. Chang, F. Hung, T. Lui, J. Mater. Res. Technol. 8 (1) (2019) 173–179.
[4] X. Chen, Y. Peng, S. Peng, S. Yao, C. Chen, P. Xu, J. Pl, One (2017) 1–28.
[5] H.J. Liu, H. Fujii, M. Maeda, K. Nogi, Sci. Technol. Weld. Join. 8 (6) (2003) 450–454.
[6] W.M. Thomas, E.D. Nicholas, J.C. Needham, M.G. Murch, P Smith, C.G. Dawes, Friction Stir Butt Welding, G.B. Patent Application No. 9125978.8.
[7] R.S. Mishra, Z.Y. Ma, Mater. Sci. Eng. R50 (2005) 1.
[8] R.S. Mishra, Z.Y. Ma, Friction stir welding and processing, Mater. Sci. Eng. R: Rep. 50 (1-2) (2005) 1–78, https://doi.org/10.1016/j.mser.2005.07.001.
[9] R.S. Mishra, Z.Y. Ma, I. Charit, Mater. Sci. Eng. A 341 (2003) 307–310.
[10] A. Chang, X.H. Du, J.C. Huang, Scr. Mater. 57 (2007) 209–212.
[11] M.L. Santella, T. Engstrom, D. Storjohann, T.-Y. Pan, Scr. Mater. 53 (2005) 201–206.
[12] A.H. Feng, Z.Y. Ma, Scr. Mater. 56 (2007) 397–400.
[13] A.G. Rao, B.R.K. Rao, V.P. Desmukh, A.K. Shah, B.P. Kashyap, Mater. Lett. 63 (2009) 2628–2630.
[14] Z.Y. Ma, Metall. Mater. Trans. A Phys. Metall. Mater. Sci. 39 (2008) 642–658.
[15] T.R. McNelley, S. Swaminathan, J.Q. Su, Recrystallization mechanisms during friction stir welding/processing of aluminum alloys, Scr. Mater. 58 (5) (2008) 349–354, https://doi.org/10.1016/j.scriptamat.2007.09.064.
[16] Z.Y. Ma, S.R. Sharma, R.S. Mishra, Effect of friction stir processing on the microstructure of cast A356 aluminum, Mater. Sci. Eng. A 433 (1-2) (2006) 269–278, https://doi.org/10.1016/j.msea.2006.06.099.
[17] Z.Y. Ma, S.R. Sharma, R.S. Mishra, Effect of multiple-pass friction stir processing on microstructure and tensile properties of a cast aluminum–silicon alloy, Scr. Mater. 54 (9) (2006) 1623–1626, https://doi.org/10.1016/j.scriptamat.2006.01.010.
[18] K.J. Al-Fadhalah, A.I. Almazrouee, A.S. Aloraier, Microstructure and mechanical properties of multi-pass friction stir processed aluminum alloy 6063, Mater. Des. 53 (2014) 550–560, https://doi.org/10.1016/j.matdes.2013.07.062.
[19] L.B. Johannes, R.S. Mishra, Multiple passes of friction stir processing for the creation of superplastic 7075 aluminum, Mater. Sci. Eng. A 464 (1-2) (2007) 255–260, https://doi.org/10.1016/j.msea.2007.01.141.
[20] P. Xue, B.L. Xiao, Z.Y. Ma, Achieving Large-area Bulk Ultrafine Grained Cu via Submerged Multiple-pass Friction Stir Processing, J. Mater. Sci. Technol. 29 (12) (2013) 1111–1115, https://doi.org/10.1016/j.jmst.2013.09.021.
[21] F.Y. Zheng, Y.J. Wu, L.M. Peng, X.W. Li, P.H. Fu, W.J. Ding, Microstructures and mechanical properties of friction stir processed Mg–2.0Nd–0.3Zn–1.0Zr magnesium alloy, J. Magnesium Alloys 1 (2) (2013) 122–127, https://doi.org/10.1016/j.jma.2013.06.001.
[22] B.o. Li, Y. Shen, W. Hu, Surface nitriding on Ti–6Al–4V alloy via friction stir processing method under nitrogen atmosphere, Appl. Surf. Sci. 274 (2013) 356–364, https://doi.org/10.1016/j.apsusc.2013.03.060.
[23] M. El Rayes, E.A. El-Danaf, The influence of multi-pass friction stir processing on the micostructural and mechanical properties of Aluminum Alloy 6082, J. Mater Process. Technol. 212 (5) (2012) 1157–1168.
[24] S.S. Mirjavadi, M. Alipour, A. Hamouda, A. Matin, S. Kord, B.M. Afshari, P.G. Koppad, Effect of multi-pass friction stir processing on the microstructure, mechanical and wear properties of AA5083/ZrO2 nanocomposites, J. Alloy. Compd. 726 (2017) 1262.
[25] E. Moustafa, Effect of multi-pass friction stir processing on mechanical properties for AA2024/Al2O3 nanocomposites, Materials 10 (2017) 1053.
[26] M. Hajizamani, M. Alizadeh, Modification of microstructure and mechanical properties of Al–Zn–Mg/3 wt.% Al2O3 composite through semi-solid thermomechanical processing using variable loads, Int. J. Mater. Res. 108 (2017) 840.
[27] M. Mhedhbi, M. Khlif, C. Bradai, J. Mater. Environ. Sci. 8 (8) (2017) 2967–2974.
[28] M.D. Sameer, A.B. Kumar, J. Mag. Alloys 7 (2019) 264–271.
[29] M.M. El-Rayes, E.A. El-Danaf, The influence of multi-pass friction stir processing on the microstructural and mechanical properties of Aluminum Alloy 6082, J. Mater. Process. Technol. 212 (5) (2012) 1157–1168, https://doi.org/10.1016/j.jmatprotec.2011.12.017.
[30] S.R. Sharma, Z.Y. Ma, R.S. Mishra, Scr. Mater. 51 (2004) 237–241.
[31] R.S. Mishra, P.S. De, N. Kumar, Friction Stir Welding and Processing, Switzerland: Springer International Publishing, 2014.
[32] S. Mabuwa, V. Msomi, Mater. Today Proc. 26 (2) (2020) 193–199.
[33] S. Mabuwa, V. Msomi, Adv. Mater. Sci. Eng. 2019 (2019) 1–15.
[34] S. Tutinchilar, G.M.K. Besharati, M. Haghpanahi, P. Asadi, Mater. Sci. Eng. A 534 (2012) 557.
[35] S. Mabuwa, V. Msomi, J. Mater. Res. Technol. 9 (5) (2020) 9632–9644.
[36] S. Mabuwa, V. Msomi, Eng. Fail. Analy. 118 (2020) 104876.